Polym. Bull. (2015) 72:2739–2756
DOI 10.1007/s00289-015-1433-1

ORIGINAL PAPER

Radiation synthesis and characterization of Poly(butyl methacrylate/acrylamide) copolymeric hydrogels and heparin controlled drug release

M. B. El-Arnaouty[1] · A. M. Abdel Ghaffar[1] · Maysara E. Aboulfotouh[1] · N. H. Taher[1] · Ahmed A. Taha[2]

Received: 6 January 2015 / Revised: 21 April 2015 / Accepted: 4 June 2015 /
Published online: 15 June 2015

Abstract Radiation-induced copolymerization of butyl methacrylate/acrylamide has been investigated. It was observed that as the irradiation dose increases, the gelation percent increases and the maximum gelation % was achieved at irradiation dose of 30 kGy. The equilibrium swelling studies of the prepared hydrogels at various conditions were carried out in an aqueous solution. The pH sensitivity in the range of 4–7.5 was investigated. It is found that the swelling behavior of Poly (BMA/AAm) is higher than that of Poly(BMA) and Poly(AAm). Swelling kinetics and diffusion mechanism indicate that the water penetration obeys non-Fickian transport mechanism. The characterization and some selected properties of the prepared hydrogels were evaluated using FTIR, XRD, TGA and SEM. The drug release characteristics of the prepared hydrogel were studied using heparin as example of anticoagulant drug. The drug release found to be governed by multiple factors contributed by each composition of the prepared hydrogel including their drug binding affinities and water uptake rates.

Keywords Radiation · Butyl methacrylate · Diffusion mechanism · Heparin controlled release

Introduction

Controlled drug release hydrogels are designed to deliver therapeutical drugs to desirable sites at appropriate time [1]. In recent years, stimuli-sensitive polymers that respond to changes in environmental conditions, such as pH, temperature, salt,

✉ A. M. Abdel Ghaffar
am_abdelghaffar@yahoo.com

[1] National Center for Radiation Research and Technology, Atomic Energy Authority, P.O. Box 29, Nasr City, Cairo 11731, Egypt

[2] Department of Chemistry, Women's College, Ain Shams University, Cairo, Egypt

light, biomolecules, and electromagnetic field [2], have received extensive attention for their unique advantages in applications for controlled drug delivery and so-called intelligent biomaterials. The release of drugs from the smart delivery systems can be triggered by the specific environments of some organs, intracellular space, or pathological sites, leading to an enhanced specificity of drug delivery and less side effects [3]. In addition to intelligent drug release behaviors, drug carriers with good biocompatibility and appropriate biodegradability are preferred in practical applications [4].

Ionizing radiation has long been recognized as a very suitable tool for synthesis of hydrogels [5, 6]. Ionizing radiation is considered as a controlled process, that can be used in preparation and sterilization of different hydrogels in one technological step, that there is no necessity to add any initiators, crosslinkers, etc., which are possibly harmful and difficult to remove. This makes radiation method is good choice in the synthesis of hydrogels, especially for biomedical use. Also from the point of view of radiation chemistry, crosslinking of polymers, including hydrogel formation, belongs to the most successful applications of this branch of science.

Few researches found in chemical copolymerization of acrylamide with butyl methacrylate hydrogel preparation [7–11]. The present work has focused on radiation synthesis of hydrogel based on butyl methacrylate and acrylamide individually and binary system. Also the details of their swelling and diffusion characteristics as their response to external stimuli such as pH were investigated. The drug release characteristics of the prepared hydrogel were studied using heparin as example of anticoagulant drug.

Experimental

Preparation of Poly(BMA/AAm) hydrogels

Butyl methacrylate, acrylamide (both with concentration 50 wt%) and (BMA/AAm) with comonomer composition (50:50 wt%) all dissolved separately in dimethyl formamide (DMF) then transferred into test tubes and gamma irradiated for preparation of Poly(butyl methacrylate), Poly(acrylamide) and Poly(butyl methacrylate/acrylamide) hydrogels, respectively. The irradiation facility was constructed by National Center for Radiation Research and Technology, Cairo, Egypt (Scheme 1).

Gelation percent

The prepared hydrogels were cut into small discs, dried and weighed. The samples were extracted by hot distilled water at 80 °C for 8 h and then dried at 40 °C until a constant weight. The gelation percent (G %) was calculated gravimetrically using the following equation:

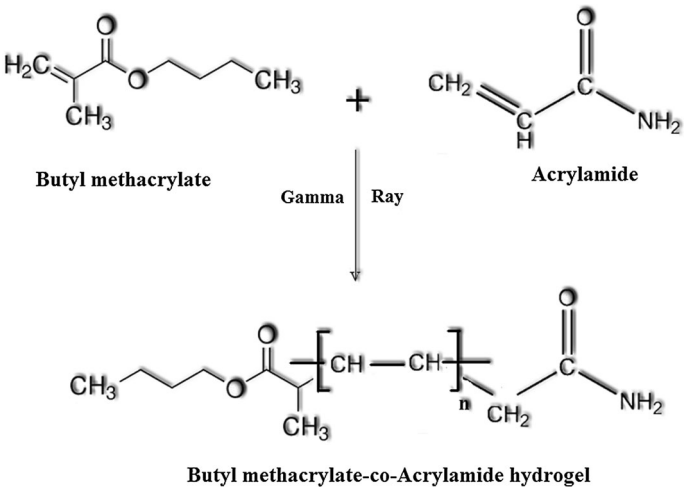

Scheme 1 Represent the copolymerization of butyl methacrylate-co-acrylamide hydrogel by gamma radiation

$$\text{Gel fraction } = \frac{W_{\text{d}}}{W_{\text{o}}} \times 100 \tag{1}$$

where W_{d} and W_{o} were the weight of dried sample after and before extractions, respectively.

Swelling studies

Equilibrium swelling

The hydrogel discs were soaked in distilled water at room temperature. Swollen gels removed from water, dried and weight for several time. The measurements were continued until a constant weight was obtained for each sample (1500 h). The weight swelling ratios percent (Q) at equilibrium was calculated using the following equation:

$$Q = \text{ Equilibrium swelling} = \frac{W_t - W_d}{W_t} \times 100 \tag{2}$$

where W_{d} is the weight of dried hydrogels and W_{t} is the weight of the swelling gel at equilibrium.

Swelling behavior at different pHs

The prepared hydrogel discs were soaked in buffer solution for (490 h) at different pHs (4, 5 and 7.5) using buffer solution composed of citric acid/trisodium citrate and sodium hydrogen phosphate/disodium hydrogen phosphate at 25 °C. The swelling percent (S %) was determined from Eq. (2).

Kinetic study of swelling

The progress of the water uptake process was monitored by determining the swelling ratio of the hydrogel as increasing at desired time intervals. For kinetic analysis of the results, Fick's law was applied. The classifications of the diffusion of water into the hydrogel are:

(i) Case I or Fickian diffusion occurs when the rate of diffusion is much less than that of relaxation. When the hydrogel swells in the water, the swollen hydrogel follows Fick's law. Thus, the rate of swelling by Case I systems is dependent on $t^{1/2}$ and the diffusion constant $n = 0.5$.
(ii) Case II diffusion (relaxation-controlled transport) occurs when diffusion is very rapid compared with the relaxation process. In Case II systems, diffusion of water through the hydrogel is rapid compared with the relaxation of polymer chains. Thus, the rate of water penetration is controlled by the polymer relaxation ($n = 1$).
(iii) Non-Fickian or anomalous diffusion occurs when the diffusion and relaxation rates are comparable. Swelling depends on two simultaneous rate processes, water migration into the hydrogel and the relaxation of polymer chains ($1 > n > 0.5$)

The swelling/diffusion kinetic parameters, as diffusion coefficients (D), swelling rate constant, diffusion constant (n) and maximum equilibrium swelling ratio, were calculated using the dynamic swelling ratio values for the prepared hydrogels by the following equations:

$$F = (M_t/M_\infty) = Kt^n. \tag{3}$$

In the above equation, F is a fraction of swelling due to the water uptake, M_t are the adsorbed water at time t and M_∞ are the adsorbed water at equilibrium, K is the swelling constant, and n is the swelling exponent.

This equation was applied to the initial stages of swellings, and plots of (ln F) versus (ln t) are shown in Fig. 5a, b, n and K were calculated from the slop and intercept of the line, respectively, it is represented in Table 2 as a function of the different pHs.

Fick's first and second laws of diffusion adequately describe the most diffusion processes. For the prepared hydrogel, the integral diffusion is given in the following equation:

$$F = M_t/M_\infty = 4\left(Dt/\Pi L^2\right)^{0.5} \tag{4}$$

where D is the diffusion coefficient and L is the thickness of the sample. In Eq. (4), the slope of linear plot between (M_t/M_∞) and $t^{1/2}$ yields diffusion coefficient D.

FTIR spectroscopic measurements

FTIR spectra were determined for the hydrogel using FTIR 6300, Jasco, made in Japan in the range 400–4000 cm^{-1}.

Thermogravimetric analysis (TGA)

TGA-50 Shimadzu, thermogravimetric analyzer (made in Japan) was used for the measurements of TGA. The nitrogen flow rate was 20 mL/min and the heating rate was 10 °C/min from ambient temperature up to 600 °C.

X-ray diffraction (XRD)

X-ray diffraction measurements were carried out for the prepared hydrogels at room temperature, X-ray diffraction pattern was recorded in the range of diffraction angle 2θ on Philips Pw 1730, and X-ray generator was equipped with scintillation counter. The diffraction patterns were run with nickel filter (Cukα). $\lambda = 1.45$ Å. The X-ray diffractograms were obtained using the following experimental condition: Filament current = 28 mA, voltage = 40 kv, and scanning speed = 20 mm/min.

Scanning electron microscopy (SEM)

JEOL-JSM-5400 scanning electron microscope (made in Japan) was used for investigating the pores structure and morphology of different hydrogels at high magnification and resolution by means of energetic electron beam, before examination the swollen hydrogels were freeze-dried using freeze dryer Modulyo product from Jencons (scientific limited, England) and then coated with gold under sputter.

Controlled release of heparin from hydrogels

Heparin loading

Heparin was loaded into different hydrogels by immersing the dry hydrogel discs (1 mm thickness, 5 mm diameter and about 0.1 g weight) in Heparin solutions which prepared using 1 mL of heparin sodium salt (which produced by ELNILE pharmaceutical company) in 10 mL distilled water for each weighted hydrogel and at pH = 7.4. Heparin was loaded into the hydrogels at the ambient temperature for 10 days. Before the immersion in the release medium, the weights of the discs were measured.

Loading percent was calculated as:

$$\text{Load } \% = \frac{W_{\text{drug}}}{W_{\text{polymer}} + W_{\text{drug}}} \times 100. \quad (5)$$

Heparin release

Heparin release from disc-shaped samples was conducted at ambient temperature and pH = 7.4. Swollen discs were taken out of the loading solution and immersed directly in the release medium of 10 mL buffer solution at pH = 7.4. The amount of released heparin was measured by the UV–Vis spectrophotometer every 30 min using the calibration curve at $\lambda_{max} = 220$ nm.

Ultraviolet spectroscopy (UV)

Determination of the heparin concentration was carried out using Milton Rot Spectronic 1201 spectrophotometer at $\lambda_{max} = 220$ nm.

Results and discussion

Effect of irradiation dose on gelation %

The effect of the irradiation dose on the gelation % is shown in Fig. 1a and the effect of different comonomer concentrations is shown in Fig. 1a, b. The observed results show that as the irradiation dose increases the gelation percent (*G* %) increases. This behavior may be attributed to the increase in the available free radical concentration and higher degrees of crosslinking of the hydrogel structure during copolymerization process [12, 13]. It was found that the optimum value of the gelation percent (*G* %) occurred at irradiation dose 30 kGy, Then, the gelation (%) was slightly decreased by increasing irradiation dose at 40 kGy, the gelation (%). This can be attributed to the degradation of the crosslinking by effect of high irradiation dose, where the rate of radiation degradation may be faster than that of radiation crosslinking [14, 15]. From Fig. 1b, it was observed that as the comonomer concentration increases, the gelation percent increases till level off at 60 wt%. This is may be due to above comonomer concentration 60 wt% the solution become viscous and the formation of homopolymers Poly(AAm) and

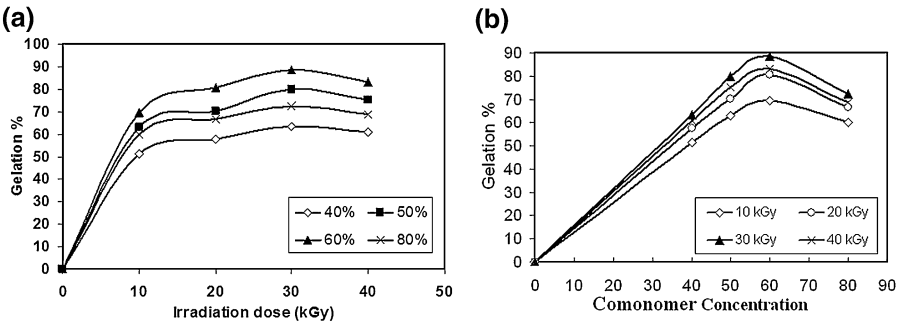

Fig. 1 Effect of **a** irradiation dose and **b** comonomer concentration on the gelation (%) of Poly(BMA/AAm) (50:50) hydrogel at different comonomer concentrations and different irradiation doses kGy

Poly(BMA) is faster than the copolymerization process where the formed free radical upon irradiation recombine which each other to form homopolymers than formation of Poly(BMA/AAm) [16–18].

Swelling behavior

Figure 2a represents the equilibrium swelling behavior of Poly(BMA/AAm) which calculated by Eq. (2) as a function of time at different irradiation doses. It was found that the swelling behavior decreases with the increase of irradiation dose, this is due to increasing the crosslinking density which leads to narrow the pore size and reduces the free spaces available for water retention [19]. Figure 2b represents the swelling behavior of Poly(BMA/AAm) prepared at 20 kGy as a function of time at different comonomer concentrations, it was found that the optimum comonomer concentration is 50 wt% that it reach to the maximum swelling percent. The swelling behavior continuously decreases with increasing the comonomer

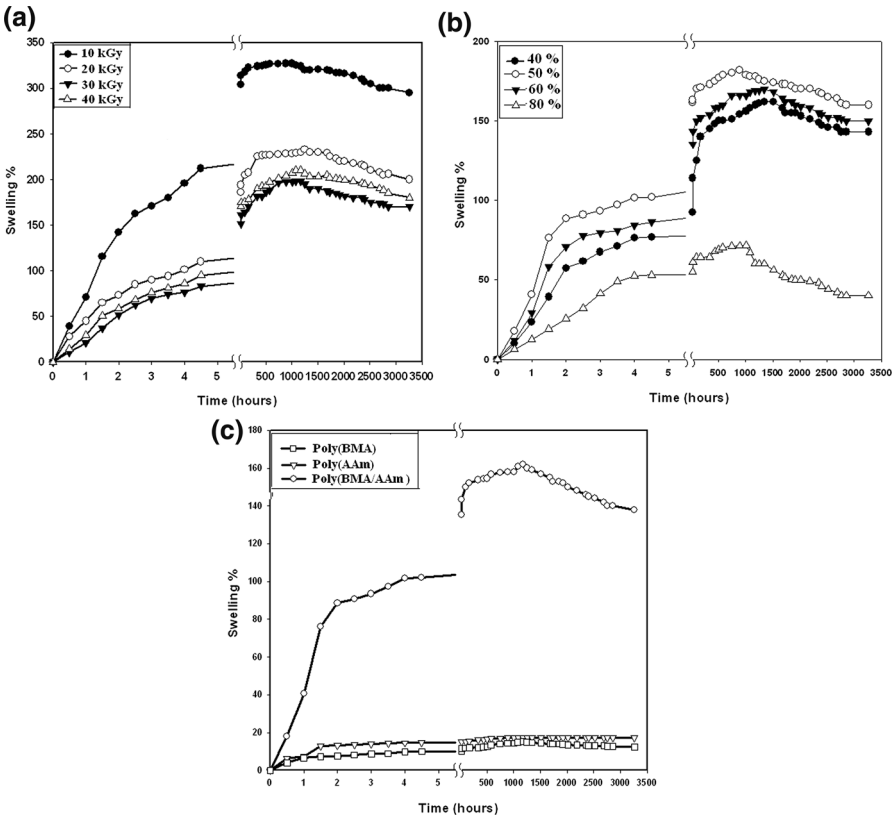

Fig. 2 The swelling behavior of **a** Poly(BMA/AAm) as a function of time at different irradiation doses, **b** Poly(BMA/AAm) as a function of time at different comonomer concentrations and **c** swelling behavior of Poly(BMA), Poly(AAm) and Poly(BMA/AAm)

concentration more than 50 %, this may be due to the great number of free radicals that increase the crosslinking of chains in the hydrogel network [20]. From Fig. 2c, it can be observed that the swelling behavior of Poly(BMA/AAm) with comonomer composition (50/50 wt%) is higher than that of Poly(AAm) and Poly(BMA) with comonomer concentration (50 wt%). This may be due to Poly(BMA/AAm) has much lower gelation % compared with the other two types of hydrogels as represented in Table 1.

Effect of pH on hydrogel swelling

The copolymer hydrogel undergoes significant change in its swelling capacity along with change of the pH of the external media. Figure 3 shows the equilibrium

Table 1 The gelation % of Poly(BMA), Poly(AAM) and Poly(BMA/AAM) at irradiation dose (20 kGy) and at 50 % comonomer concentration

Hydrogel	Poly(BMA)	Poly(AAM)	Poly(BMA/AAM)
Gelation %	99.322	87.73	63.513

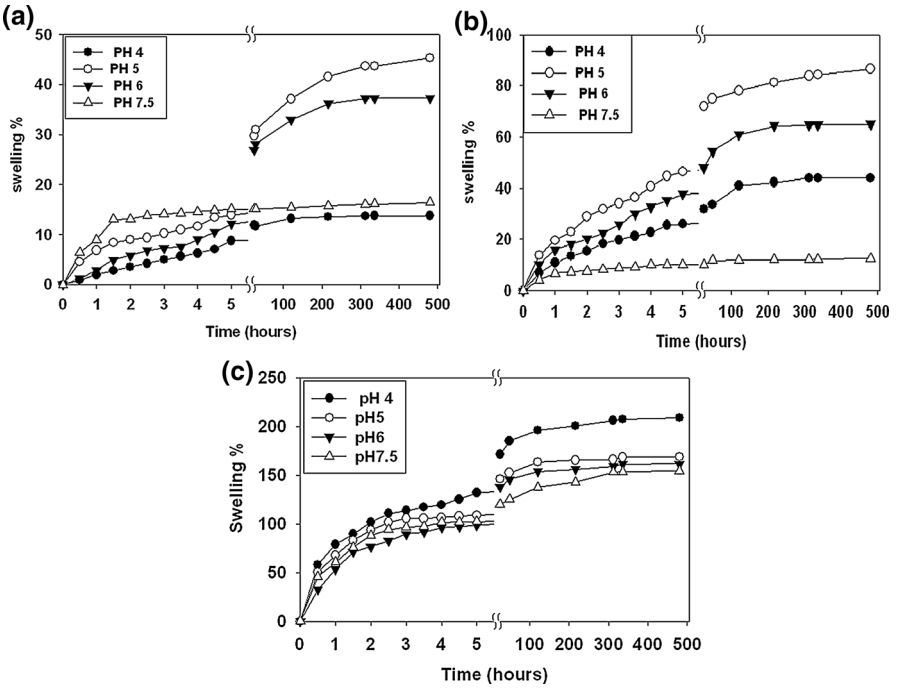

Fig. 3 Relationship between the swelling (%) and time (h) for **a** Poly(BMA), **b** Poly(AAm) at comonomer concentration 50 wt% **c** Poly(BMA/AAm) at comonomer composition (50/50 wt%), and at different pHs

swelling behavior of the Poly(BMA), Poly(AAm) and Poly(BMA/AAm) hydrogels, respectively, in buffer solution of different pHs (4, 5, 6, and 7.5). The results indicate that the hydrogels show low swelling at pH 7.5. This may be due to unionized butyl methacrylate and amide groups which led to low osmotic swelling pressure and compact hydrogen bonding interactions which restricts the water entrance [21].

However, when the hydrogels were placed in the medium of lower pH (4, 5), the ionization of the amide group ($O{=}C{-}NH^{+3}$) not only increases the osmotic swelling pressure, but it also results in relaxation of the polymeric chains due to the repulsion among similarly charged function group which contributes towards greater water uptake [22].

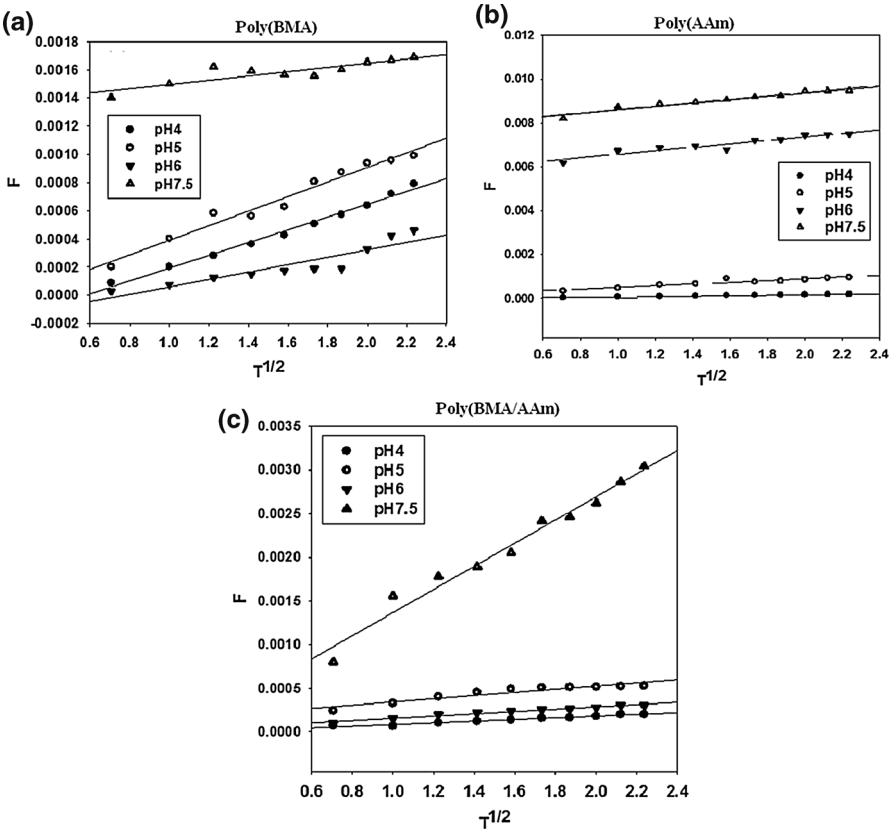

Fig. 4 Representation of fractional swelling ratio (*f*) of **a** Poly(BMA), **b** Poly(AAm) and **c** Poly(BMA/AAm) hydrogels

Swelling kinetics and diffusion mechanism

The diffusion of water into the hydrogel was classified into three different types based on the relative rates of diffusion and polymer relaxation as mentioned in experimental part [22].

Figure 4 shows the relation between time and fraction of swelling due to the water uptake. The diffusion constant (n) for the three different hydrogels Poly(BMA), Poly(AAm) and Poly(BMA/AAm) is obtained from Fig. 5a–c, the apparent diffusion coefficient D is obtained from the slope of the straight line. The D values for the three hydrogels at different pHs have been analyzed for the predication of the water transport mechanisms. The diffusion constant (n) values are reported in Table 2 together with the other swelling parameters. From the results, it can be concluded that water penetration may occur according to the non-Fickian transport mechanism, since the values of the diffusion constant (n) range between 0.5 and 1.0 [23] that the anomalous diffusion occurs when the diffusion and relaxation rates are comparable [24].

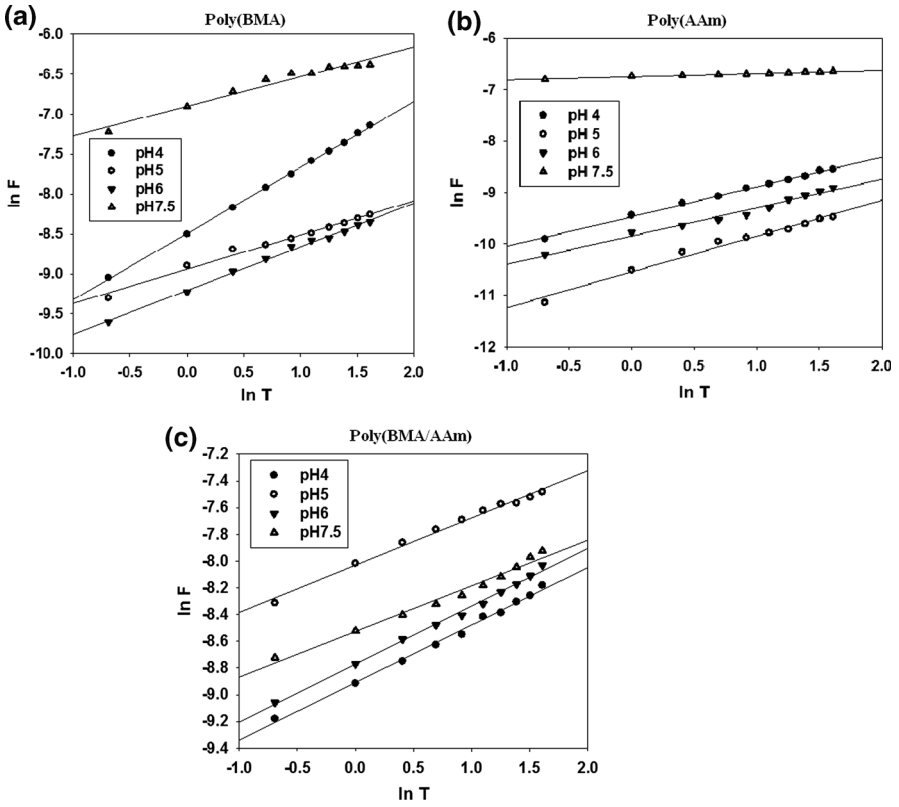

Fig. 5 Representation of fractional swelling ln(f) of **a** Poly(BMA), **b** Poly(AAm) and **c** Poly(BMA/AAm) hydrogels at time t and at different pHs (4, 5, 6 and 7.5)

Table 2 The value of swelling parameters for the different hydrogels, at different pHs and a dose 20 kGy

Different hydrogels	pH	*D*	*n*	*k*	Eq swelling (%)
Poly(BMA)	4	2.91	0.654	−9.30	13.78
	5	3.344	0.611	−9.35	41.67
	6	6.386	0.582	−9.74	36.2
	7.5	5.309	0.519	−7.25	17.5
Poly(AAm)	4	3.376	0.543	−10.03	44
	5	2.116	0.513	−11.21	102.9
	6	4.776	0.633	−10.37	65
	7.5	4.130	0.641	−6.80	15.2
Poly(BMA/AAm)	4	4.106	0.582	−9.33	226.9
	5	4.661	0.574	−8.37	126.8
	6	4.316	0.556	−9.20	165.8
	7.5	6.348	0.612	−8.86	178

It is noted that from the swelling and diffusion kinetic results of the prepared hydrogels, it depends on the degree of crosslinking where high gelation percent hydrogels are characterized by lower swelling compared to the hydrogels with lower gelation percent.

FTIR analysis

Infrared spectroscopy was carried out to identify the chemical structure of the prepared hydrogels. Figure 6a–c shows the IR spectra of Poly(BMA), Poly (AAm) and Poly(BMA/AAm) hydrogels respectively. In case of Fig. 6a for Poly(BMA), the peak observed at 1683 cm^{-1} corresponding to the C=O of the acrylate group of butyl methacrylate and the peak around 2945 and 2875 cm^{-1} for (C–H) asymmetric and symmetric in CH_3 and CH_2 group and the peak at 1440 cm^{-1} represent a bending vibration for CH_2 group.

In case of Fig. 6b for Poly(AAm), the peak around 2990 corresponds to symmetric CH_2 group and the peak at 1690 cm^{-1} corresponds to the C=O group of amide group. Also the broad peak at the range 3200–3740 corresponds to NH_2 group of Poly(AAm).

In case of Fig. 6c for Poly(BMA/AAm), the peaks at 2945 and 2875 cm^{-1} represent the (C–H) asymmetric and symmetric in CH_3 and CH_2 group, where the peaks at 1375 and 1125 cm^{-1} represent the bending vibration for CH_2 and CH_3 groups. The broad absorption band at 3233–3750 cm^{-1} indicates the introduction of the NH_2 groups onto Poly(BMA/AAm). Also, the broad peak appeared at 1683 cm^{-1}, which indicates the presence of carbonyl group of Poly(BMA/AAm).

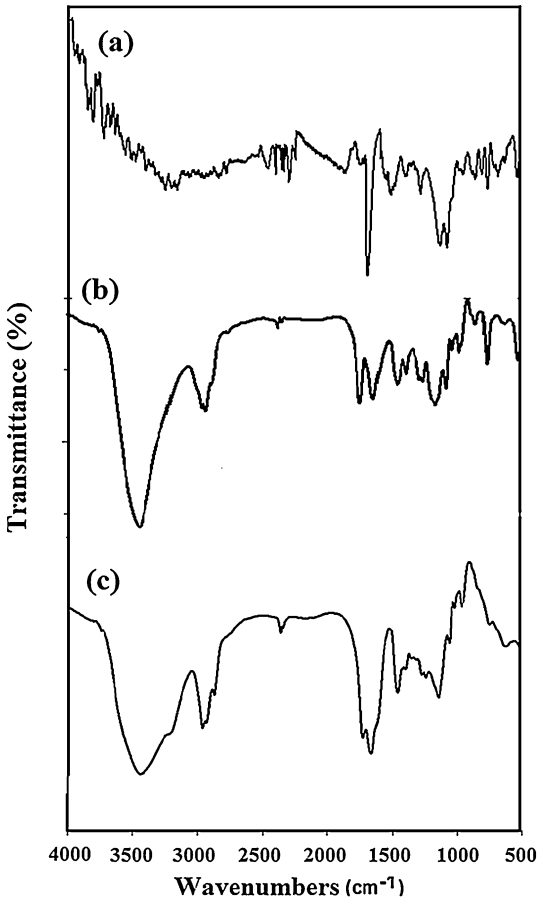

Fig. 6 FTIR spectroscopic analysis of different hydrogels prepared at 20 kGy of *a* Poly(BMA), *b* Poly(AAm) at comonomer concentration 50 % and *c* Poly(BMA/AAm) at composition (50:50 wt%) hydrogels

Thermogravimetric analysis

The TG curves and the rate of thermal decomposition (d*w*/d*t*) of the different hydrogels are shown in Fig. 7a–c. For Poly(BMA) Fig. 7a the first stage of weight loss in the range between 100 and 180 °C which corresponds to moisture loss. The second step, from 180 to 260 °C which attributed to the side chain loss, and finally back have degradation at range between 260 and 470 °C with maximum loss at 400 °C.

The thermal degradation of the Poly(AAm) occurs via three-stage process which represent in Fig. 7b. The first stage of weight loss in the range between 100 to 150 °C which may be attributed to the elimination of adsorbed moisture via dehydration. The second stage of weight loss in the range from 150 to 230 °C corresponds to the loss of ammonia [25]. The third stage occurred between 230 and 400 °C with a maximum weight loss rate at 300 °C which attributed to the main chain scission process and complete depolymerization occurs.

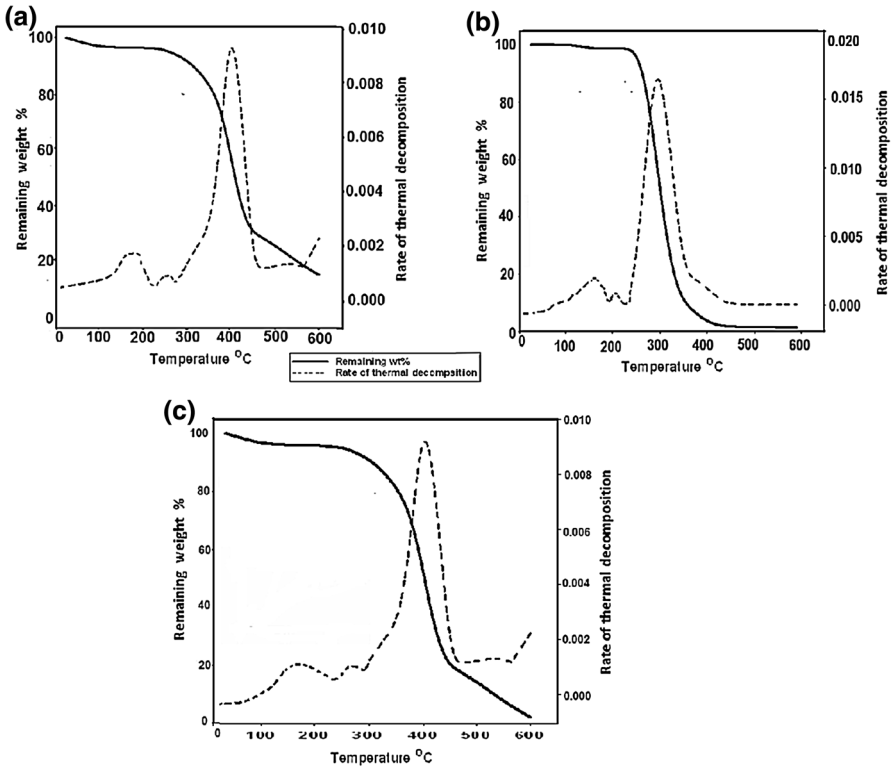

Fig. 7 TGA curves and the rate of thermal decomposition (d*w*/d*t*) versus the decomposition temperature for **a** Poly(BMA), **b** Poly(AAm) hydrogels, **c** Poly(BMA/AAm)

Figure 7c shows the thermal degradation of Poly(BMA/AAm) the first stage of weight loss in the range between 100 and 170 °C which corresponds to the elimination of moisture. The second step, from 170 to 250 °C which attributed to the side chain loss, and finally third-stage degradation at range between 250 and 460 °C with maximum loss rate at 400 °C [25]. In a comparison, the Poly(BMA) and Poly(BMA/AAm) hydrogels have slightly higher thermal stability than Poly(AAm) and they degraded in a similar manner.

X-ray study

Figure 8a–c shows the X-ray diffractogram for Poly(BMA), Poly(AAm) and Poly(BMA/AAm) hydrogels, respectively. From Fig. 8a–c, it was found that the structure morphology of Poly(BMA/AAm) hydrogel shown in Fig. 8c has a different character than the original Poly(BMA) and Poly(AAm). The intensity of the peak of Poly(BMA/AAm) decreased and becomes more broad, therefore, crystallinity decreased. This is due to the combination between partially hydrophobic monomer (BMA) and partially hydrophilic AAm where the

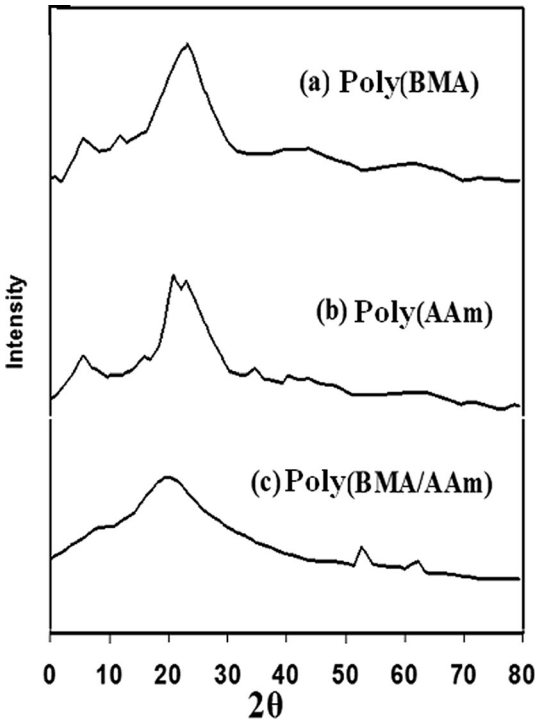

Fig. 8 XRD for *a* Poly (BMA), *b* Poly (AAm) and *c* Poly (BMA/AAm)

combination increases the pore size which leads to disordering of the structure that causes a drop in the degree of ordering of the formed hydrogel Poly(BMA/AAm).

Scanning electron microscope (SEM)

The scan electron microscope shows the morphology and the pore size of different hydrogels. In our study, the observed results confirm the porous structure which had resulted from the expanded structure after the swollen hydrogel samples were freeze-dried.

Figure 9a–c represents the images of Poly(BMA), Poly(AAm) and Poly(BMA/AAm) hydrogels, respectively. It shows that the surface and morphology of the prepared hydrogels are not smooth, where many globules and flaky structures are observed.

The copolymerization of BMA and AAm increases the amount of pores of the hydrogel due to the presence of carboxylate anion group of butyl methacrylate BMA and amide group of AAm. The results are attributed to our mentioned results in the swelling study that a highly expanded network can be formed by electrostatic repulsions among the butyl methacrylate carboxylate anions ($-COO^-$) during the polymerization process [26].

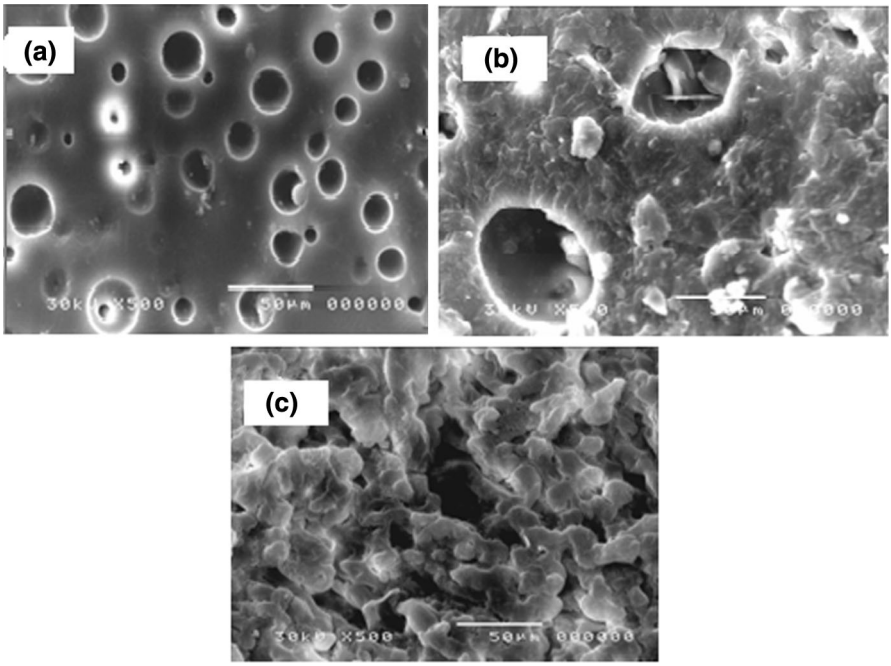

Fig. 9 Scanning electron micrograph of **a** Poly(BMA), **b** Poly(AAm) at concentration 50 wt% and **c** Poly(BMA/AAm) at (50:50) wt% comonomer composition, irradiation dose 20 kGy

Heparin controlled release from the prepared hydrogels

The objective of this study is using of the prepared hydrogels as heparin controlled release polymers for the prevention of surface-induced thrombosis. Surface-induced thrombosis occurs when a polymer surface contacts blood, stimulating the intrinsic clotting pathway. One method to improve the properties of a blood contacting surface is the application of heparin controlled release polymers [27, 28].

Heparin loading studies

Figure 10 shows that the heparin loading % of Poly(BMA/AAm) hydrogel is much higher than that of both Poly(BMA) and Poly(AAm) hydrogels. Loading percent will directly depend on the swelling properties of the prepared hydrogels [29], where Poly(BMA/AAm) hydrogel exhibits more swelling percent than that of both Poly(BMA) and Poly(AAm) hydrogels. This is due to the combination between partially hydrophobic monomer (BMA) and partially hydrophilic AAm that this combination increases the pore size which leads to more water diffusion towards the hydrogel matrix which leads to increase of the loading percent of the heparin in Poly(BMA/AAm).

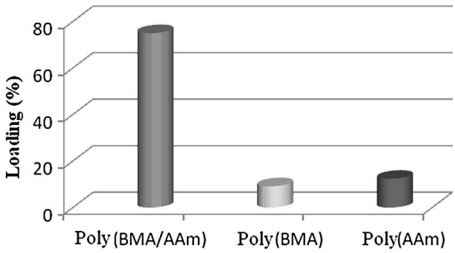

Fig. 10 The loading % values of Poly(BMA), Poly(AAm) and Poly (BMA/AAm) hydrogels

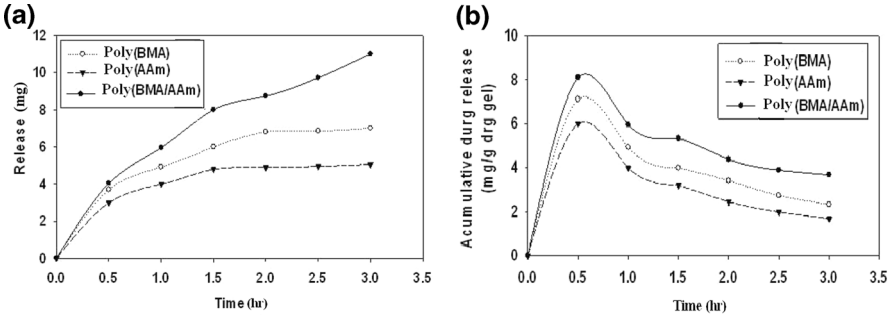

Fig. 11 **a** Heparin release from Poly(BMA), Poly(AAm) and Poly(BMA/AAm) hydrogels as a function of time (h), **b** the rate of heparin release from Poly(BMA), Poly(AAm) and Poly(BMA/AAm) hydrogels as a function of time (h)

Heparin release studies

Heparin release from the prepared hydrogels was studied as a function of time. The release profiles are represented in Fig. 11a, b. It is observed that an initial high heparin release rate up to 2 h, followed by a significant slower rate (2–3 h) for all prepared hydrogels is shown in Fig. 11. Also, it is noted that the drug release is higher for Poly(BMA/AAm) hydrogel than that of both Poly(BMA) and Poly(AAm). This is due to both lower gelation percent as shown in Table 1 and high swelling as shown in swelling studies for P(BMA/AAm) hydrogel [24]. From gelation study, moderate swelling behavior and uniform porous structure of Poly(BMA) as well as its controlled drug release. Therefore, there is a possibility to use the Poly(BMA) hydrogel loaded with heparin as example of anticoagulant drug carrier [27, 28, 30, 31].

Conclusions

It can be concluded that the prepared hydrogels by direct radiation technique have proved to be promising. The study indicating the radiation-induced polymerization is a preferable (efficient, fast and inexpensive) methodology for the fabrication of drug delivery system. The results show that the prepared materials possessed high

thermal stability and good hydrophilic properties. The drug release found to be governed by multiple factors contributed by each composition of the prepared hydrogel including their drug binding affinities and water uptake rates. Therefore, from the previous studies there is a possibility to use the Poly(BMA) hydrogel loaded with heparin as example of anticoagulant drug carrier.

References

1. He C, Zhuang X, Tang Z, Tian H, Chen X (2012) Stimuli-sensitive synthetic polypeptide-based materials for drug and gene delivery. Adv Health Mater 1:48–78
2. He C, Kim SW, Lee DS (2008) In situ gelling stimuli-sensitive block copolymer hydrogels for drug delivery. J Controlled Release 127:189–207
3. Danhier F, Feron O, Preat V (2010) To exploit the tumor microenvironment: passive and active tumor targeting of nano carrier for anticancer drug delivery. J Controlled Release 148:135–146
4. Tian H, Tang Z, Zhuang X, Chen X, Jing X (2012) Biodegradable synthetic polymers: preparation, functionalization and biomedical application. Review article. Prog Polym Sci. 37:237–280
5. Rosiak JM, Ulanski P (1999) synthesis of hydrogels by irradiation of polymer in aqueous solution. Radiat Phys Chem 140:139–151
6. Zhou Y, Zhao Y, Wang L, Xu L, Zhai M, Wei S (2012) Radiation synthesis and characterization of nanosilver/gelatin/carboxymethyl chitosan hydrogel. Radiat Phys Chem 81:553–560
7. Srinivasulu B, Raghunath RP, Sundaram EV, Srinivas M, Lalitha S (1991) Reactivity ratios and thermal and dielectric studies of copolymers of acrylamide with butyl methacrylate. Eur Polym J 27:979–981
8. Katono H, Maruyama A, Sanui K, Ogata N, Okano T, Sakurai Y (1991) Thermo-responsive swelling and drug release switching of interpenetrating polymer networks composed of poly (acrylamide-*co*-butyl methacrylate) and poly (acrylic acid). J Controlled Release 16:215–228
9. Shaofeng X, Frantisek S, Fréchet JMJ (1997) Rigid porous polyacrylamide-based monolithic columns containing butyl methacrylate as a separation medium for the rapid hydrophobic interaction chromatography of proteins. J Chromatogr A 775:65–72
10. Xiao X, Lu C (2012) Effect of mixed solvent on fabrication, morphology and monodispersity of microspheres with hydrophobic poly(butyl methacrylate) shells. J Wuhan Univ Technol Mater Sci Ed 27:048–1052
11. XiaoBo R, JianYong C, HuaPeng Z, HongYan T (2014) Effect of the polar molecule on copolymerization of butyl methacrylate/acrylamide. Sci China Technol Sci 44:99–107
12. Shem JW, Nho YC (2003) Preparation of poly (acrylic acid)/chitosan hydrogels by gamma irradiation and in vitro. J Appl Polym Sci 90:3660–3667
13. Sokker HH, Abdel Ghaffar AM, Gad YH, Aly AS (2009) Synthesis and characterization of hydrogels based on grafted chitosan for the controlled drug release. Carbohydr Polym 75:222–229
14. Hegazy EA, Abd El-Aal SE, AbuTalib MF, Dessouki AM (2004) Radiation synthesis and characterization of poly(*N*-vinyl-2-pyrrolidone/acrylic acid) and poly *N*-vinyl-2-pyrrolidone/acrylamide) hydrogels for some metal-ion separation. J Appl Polym Sci 92:2642–2652
15. El-Arnaouty MB (2010) Effect of mono and di protic on the characterization of 2-hydroxyethylmethacrylate based hydrogel prepared by γ-radiation and its application for drug delivery. J Radiat Res Appl Sci 3:763–793
16. Hegazy EA, Ishigaki I, Okamoto J (1981) Radiation grafting of acrylic acid onto fluorine-containing polymers. I. Kinetic study of preirradiation grafting onto poly(tetrafluoroethylene). J Appl Polym Sci 26:3117–3124
17. Hegazy EA, Dessouki AM, El-Dessouky MM, El-Sawy NM (1985) Crosslinked grafted PVC obtained by direct radiation grafting. Radiat Phys Chem 26:143–149
18. Sokker HH, Abdel Ghaffar AM, Nada AMA (2006) Synthesis and characterization of radiation grafted copolymer for removal of nonionic organic contaminants. J Appl Polym Sci 100:3589–3595
19. El-Hag AA, Al-Arifi A (2009) Characterization and in vitro evaluation of starch based hydrogels as carrier for colon specific drug delivery systems. Carbohydr Polym 78:725–730

20. Bajpai AK, Giri A (2003) Water sorption behavior of highly swelling (carboxymethylcellulose-*g*-polyacrylamide) hydrogels and release of potassium nitrate as agrochemical. Carbohydr Polym 53:271–279
21. Young CN, Youn ML, Young ML (2004) Preparation, properties and biological application of pH-sensitive poly(ethylene oxide) (PEO) hydrogels grafted with acrylic acid(AAc) using gamma-ray irradiation. Radiat Phys Chem 71:239–242
22. Singh B, Chauhan GS, Sharma DK, Chauhan N (2007) The release dynamics of salicylic acid and tetracycline hydrochloride from the psyllium and polyacrylamide based hydrogels (II). Carbohydr Polym 67:559–565
23. Vervoot L, Vanden Mooter G, Rombaut P, Augustijns P, Kinget R (1998) Inulin hydrogels. II. In vitro degradation. Int J Pharm 172:137–145
24. Eid M, El-Arnaouty MB (2009) Kinetic degradation an controlled drug delivery system studies for sensitive hydrogels prepared by gamma irradiation. J Appl Polym Sci 112:1745
25. Kalagasidis Krušić M, Džunuzović E, Trifunović S, Filipović J (2004) Polyacrylamide and poly (itaconic acid) complexes. Eur Polym J 40:793–798
26. Zhang GG, Zha LS, Zhou MH, Ma JH, Liang BR (2005) Preparation and characterization of pH and temperature responsive semi-interpenetrating polymer network hydrogels based on linear sodium alginate. J Appl Polym Sci 97:1931–1940
27. Gutowska A, Bae YH, Feijen J, Kim SW (1992) Heparin release from thermosensitive hydrogels. J Controlled Release 22:95–104
28. Gong F, Cheng X, Wang S, Zhao Y, Gao Y, Cai H (2010) Heparin-immobilized polymer as non-inflammatory and non- thrombogenic coating materials for arsenic trioxide eluting sents. Acta Biomater 6:534–564
29. Bastide SC, Candau S, Leibler L (1981) Osmotic deswelling of gels by polymer solution. Macromolecules. 14:719–726
30. Simon J, Carl G, Eidelman N, Kennedy SB, Sehgal A, Khatri CA, Washburn NR (2005) Combinatorial screening of cell proliferation on poly(L-lactic acid)/poly(D, L lactic acid) blends. Biomaterials. 26:6906–6915
31. Scotchford CA, Ball M, Winkelmann M, Voros J, Csucs C, Brunette DM, Danuser G, Textor M (2003) Chemically patterned, metal-oxide-based surfaces produced by photolithographic techniques for studying protein- and cell-interactions. II. Protein adsorption and early cell interactions. Biomaterials. 24:1147–1158